Protein NMR

International Edition: DOI: 10.1002/anie.201802501
German Edition: DOI: 10.1002/ange.201802501

Two Histidines in an α-Helix: A Rigid Co^{2+}-Binding Motif for PCS Measurements by NMR Spectroscopy

*Alireza Bahramzadeh, Hailun Jiang, Thomas Huber, and Gottfried Otting**

Abstract: *Pseudocontact shifts (PCS) generated by paramagnetic metal ions present valuable long-range information in the study of protein structural biology by nuclear magnetic resonance (NMR) spectroscopy. Faithful interpretation of PCSs, however, requires complete immobilization of the metal ion relative to the protein, which is difficult to achieve with synthetic metal tags. We show that two histidine residues in sequential turns of an α-helix provide a binding site for a Co^{2+} ion, which positions the metal ion in a uniquely well-defined and predictable location. Exchange between the bound and free cobalt is slow on the timescale defined by chemical shifts, but the NMR resonance assignments are nonetheless readily transferred from the diamagnetic to the paramagnetic NMR spectrum by an I_zS_z-exchange experiment. The double-histidine-Co^{2+} motif offers a straightforward, inexpensive, and convenient way of generating precision PCSs in proteins.*

Paramagnetic metal ions elicit large effects in NMR spectra, which can be used to obtain unique long-range structural information in proteins tagged with a single paramagnetic metal ion. In particular, the metal ion can cause large chemical-shift changes (pseudocontact shifts; PCS) arising from an anisotropic magnetic susceptibility ($\Delta\chi$), and the PCSs report on the coordinates of the nuclear spins in the frame of the $\Delta\chi$ tensor.[1] The extraordinary value of PCSs for 3D structure analysis of proteins has prompted the development of many different strategies to attach a paramagnetic metal ion site-specifically to otherwise diamagnetic biological macromolecules.[2,3]

The most popular method for tagging a protein with a paramagnetic metal ion relies on chemical reaction of single cysteine residues in the protein with a synthetic metal-chelating complex. This, like other approaches relying on chemical modification of the target protein, invariably results in flexible tethers between the protein and metal chelate, which leads to smaller-than-expected PCSs and compromises the validity of using a single $\Delta\chi$ tensor to interpret the PCSs observed in the protein.[4,5] Even the best double-arm tags allow the metal ion to move between locations as far apart as 15 Å.[6,7] Alternatively, proteins can be mutated to create an artificial metal-binding site. For example, lanthanide-binding peptide motives have been inserted into polypeptide loops of the target protein.[8,9] This approach immobilizes the metal ion well, but constitutes a major modification of the protein and requires prior knowledge of the 3D structure of the protein. The quest for a rigid metal probe that is broadly applicable and generates significant PCSs prompted us to investigate the potential of the double-histidine (dHis) motif that has previously been used as a copper-binding motif for protein purification,[10] distance measurements by electron paramagnetic resonance (EPR) spectroscopy,[11–13] and measurements of paramagnetic relaxation enhancements (PRE) by NMR spectroscopy.[14] The dHis motif binds a single Cu^{2+} ion between the imidazole rings of two histidine residues (Figure 1). Since Cu^{2+} generates large paramagnetic relaxation enhancements (PRE) and only very small PCSs, we explored the utility of the dHis motif for binding a high-spin Co^{2+} ion, which is known to produce fairly large PCSs and relatively small PREs. The expectation was that good metal immobilization would result in a sizeable magnetic susceptibility anisotropy ($\Delta\chi$) tensor that is directly proportional to the alignment tensor caused by paramagnetically induced molecular alignment with the magnetic field.[15] Molecular alignment results in residual dipolar couplings (RDC) that contain very detailed structural information across the entire molecule[16] and it would be convenient if the alignment tensor could simply be derived from the $\Delta\chi$ tensor, since PCSs are more easily measured than RDCs. For conventional, flexible metal tags, the distance dependence of PCSs spoils the proportionality between the $\Delta\chi$ and alignment tensors.[5]

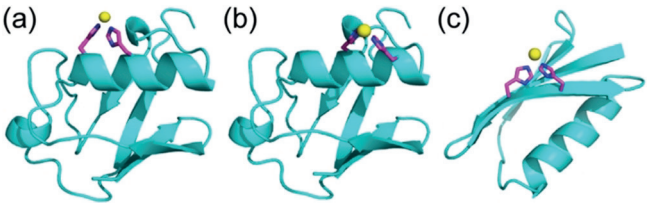

Figure 1. The Co^{2+} binding site generated by two histidine side chains. a) Ribbon representation of human ubiquitin with histidine residues modeled at positions 24 and 28 (mutant E24H/A28H). The yellow sphere indicates Co^{2+} ion binding to the dHis motif. b) Same as (a) but for the mutant A28H/D32H. c) The dHis motif grafted onto a β-strand of GB1 (mutant E15H/T17H).

Two versions of the dHis motif have been reported.[10,12] In the first version, two histidine residues are placed into two neighboring turns of an α-helix (positions i and $i+4$). This α-helical dHis motif localizes the metal ion well because a histidine side-chain contains only two rotatable bonds and simultaneous coordination of the metal ion by two histidine side-chains is possible only if the χ_1 angles of the residues in

[*] A. Bahramzadeh, H. Jiang, Prof. T. Huber, Prof. G. Otting
Research School of Chemistry, The Australian National University
Canberra, ACT 2601 (Australia)
E-mail: gottfried.otting@anu.edu.au

Supporting information and the ORCID identification number(s) for the author(s) of this article can be found under: https://doi.org/10.1002/anie.201802501.

positions i and $i+4$ are near 180° and −60°, respectively. In the second version, the histidine residues are placed in positions i and $i+2$ of an extended β-strand.

To test the performance of the dHis motif with a Co^{2+} ion, we prepared the double mutants E24H/A28H and A28H/D32H of ubiquitin as examples of the α-helical dHis motif, and the mutant E15H/T17H of the protein GB1 as an example of a β-strand dHis motif. The uniformly ^{15}N-labeled proteins were expressed in *E. coli* and purified by taking advantage of the metal-binding affinity of the double-His motif. Previously, the dHis motif has been shown to allow purification on a column derivatized with Cu^{2+}-iminodiacetate (Cu-IDA).[10] We found that the proteins could also readily be purified on a conventional Ni^{2+} nitrilotriacetate (Ni-NTA) column without an additional His tag. Any metal bound to the final protein samples was removed by dialysis against an EDTA buffer.

Isothermal calorimetry showed dissociation constants of cobalt from the dHis motifs of about 40 μM for ubiquitin E24H/A28H, 85 μM for ubiquitin A28H/D32H, and 180 μM for GB1 E15H/R17H (Figure S1 in the Supporting Information).

To verify the location of the Co^{2+} ion with respect to the protein, we measured PCSs in [^{15}N,^{1}H]-HSQC spectra, preparing paramagnetic samples by titrating $CoCl_2$ and diamagnetic reference samples with $ZnCl_2$ (Figure 2A and Figure S3). The titration with $CoCl_2$ yielded a set of new cross-peaks, thus indicating that the exchange between protein with and without bound Co^{2+} ion is slow on the NMR timescale. The exchange rate between bound and free Co^{2+} was measured by N_z-exchange spectra[18] of samples prepared with substoichiometric amounts of $CoCl_2$. The exchange rates were found to be about 50 s^{-1}. This relatively fast rate allowed the use of short mixing times in I_zS_z-exchange experiments, which can be recorded with a simpler and shorter pulse sequence.[17] In this spectrum, exchange cross-peaks identify corresponding pairs of peaks in the diamagnetic and paramagnetic protein (Figure 2B),[17,19] thereby facilitating the transfer of the assignments from the diamagnetic to the paramagnetic protein. To the best of our knowledge, this method of assigning paramagnetic NMR spectra has been reported only twice before: for the special case of a protein with a natural metal binding site[18] and for a ubiquitin mutant ligated with an IDA tag.[20] In the case of the IDA tag, exchange cross-peaks were observed only with long mixing times and were not observable in another protein.[21] The faster exchange rate associated with the dHis-Co^{2+} motif extends this strategy to a wider range of proteins.

Using the measured PCSs, the program Numbat[22] was used to fit $\Delta\chi$ tensors to different published 3D structures of ubiquitin (Table S1). Excellent correlations between back-calculated and experimental PCSs were obtained for the ubiquitin mutants E24H/A28H and A28H/D32H (Figure 3a,b). In contrast, the fit obtained for GB1 E15H/T17H was of lesser quality and the $\Delta\chi$ tensor was of smaller magnitude (Table S1), thus suggesting a less well localized metal position. Importantly, the $\Delta\chi$ tensor fits always located the metal ion at the expected position between the histidine side chains of the dHis motif (Figure 3e,f). This is the first time that the metal position has been confirmed experimentally for a dHis-metal complex.

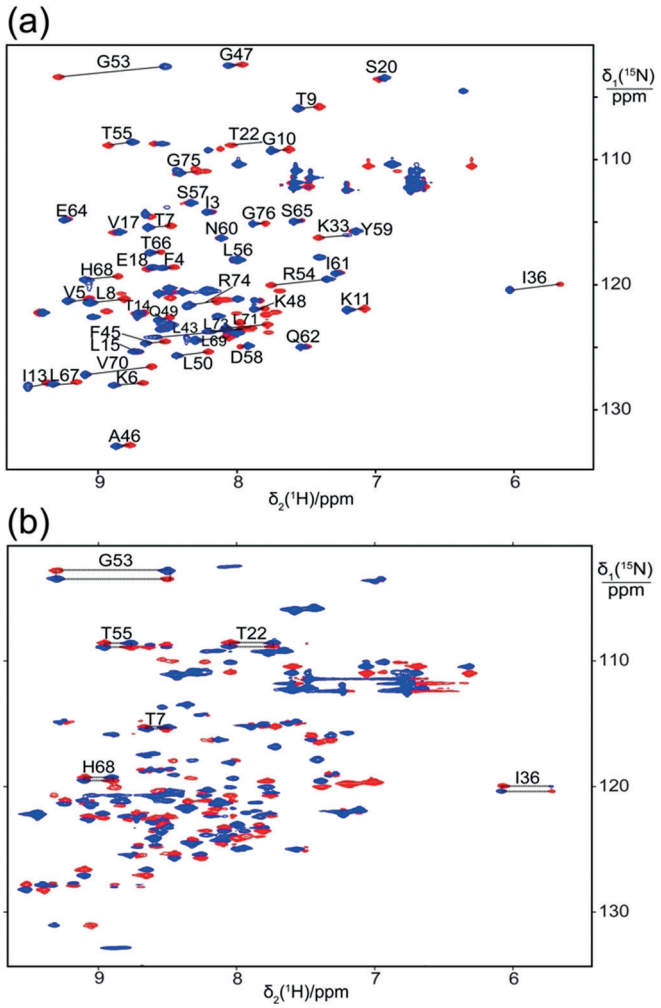

Figure 2. PCSs induced by a Co^{2+} ion bound to the dHis motif of ubiquitin E24H/A28H. All NMR spectra were measured at 25 °C on a Bruker 800 MHz NMR spectrometer equipped with a TCI cryoprobe. a) Superimposition of [^{15}N,^{1}H]-HSQC spectra of 0.8 mM solutions of uniformly ^{15}N-labeled protein in NMR buffer (20 mM MES, pH 6.5) with $ZnCl_2$ (diamagnetic reference, red cross-peaks) or $CoCl_2$ (paramagnetic spectrum, blue cross-peaks) in equimolar ratios. Assignments are shown for cross-peaks of backbone amides with significant PCSs. b) I_zS_z-exchange spectrum[17] recorded with 0.5 equivalents of Co^{2+} ions, using an exchange time of 6 ms. Exchange peaks (red) connect the auto peaks (blue) of protein with and without bound cobalt. Exchange peaks have the opposite sign from auto peaks and allow the unambiguous transfer of the peak assignments from the diamagnetic protein to the paramagnetic sample. For selected residues, the resulting rectangular set of cross-peaks is marked with the assignment.

If the metal ion is well localized, the paramagnetism is correctly described by a single $\Delta\chi$ tensor and the axial and rhombic components of the paramagnetically induced alignment tensor A become directly proportional to those of the $\Delta\chi$ tensor [Eq. (1)]:

$$A_{ax,rh} = (B_0^2/15\mu_0 k_B T)\Delta\chi_{ax,rh} \quad (1)$$

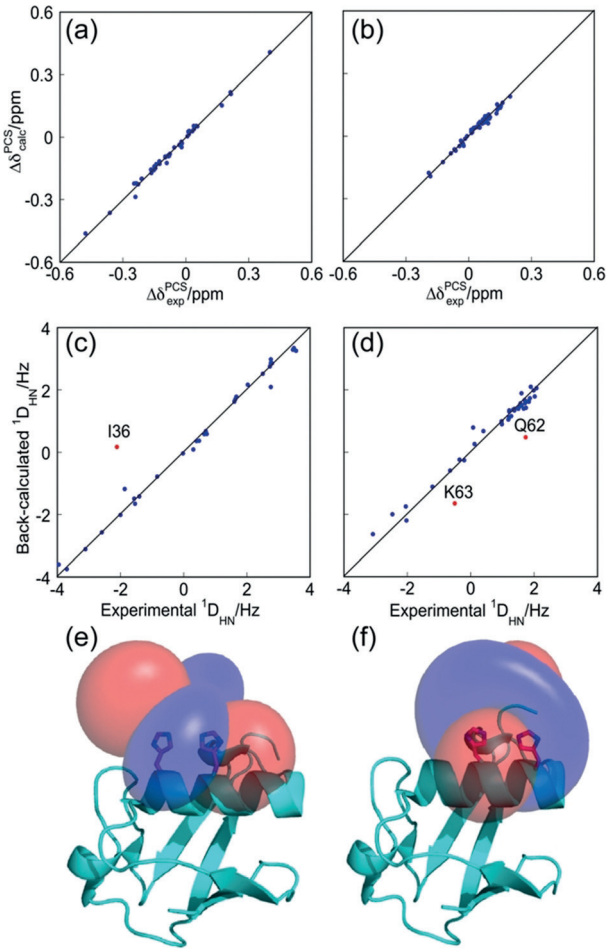

Figure 3. Correlation between back-calculated and experimental PCSs and RDCs in human ubiquitin with the dHis motif. The $\Delta\chi$ tensor fits used the experimental PCSs with a published structure ensemble (PDB ID: 2KOX[23]). Alignment tensors used for back-calculating RDCs were assumed to be proportional to the $\Delta\chi$ tensors [Eq. (1)]. a) PCS correlation for ubiquitin E24H/A28H. b) PCS correlation for ubiquitin A28H/D32H. c) RDC correlation for ubiquitin E24H/A28H. An outlier (Ile36) is highlighted by a red point. d) RDC correlation for ubiquitin A28H/D32H. Two outliers highlighted in red. e) PCS isosurfaces representing the $\Delta\chi$ tensor plotted on the 3D structure of ubiquitin. The isosurfaces correspond to PCSs of 1 ppm (blue) and −1 ppm (red) generated by the dHis-Co^{2+} motif of ubiquitin E24H/A28H. The backbone of the protein is drawn in a ribbon representation (cyan) and the histidine side chains of the double-His motif are indicated by lines. f) Same as (e) but for ubiquitin A28H/D32H. A similar tensor orientation was also observed in an α-helical dHis-Co^{2+} motif installed in another protein (Figure S5).

where B_0 is the magnetic field strength, μ_0 the magnetic susceptibility of vacuum, k_B the Boltzmann constant, and T the temperature. To test this relationship, we measured $^1D_{NH}$ RDCs for backbone amides of the cobalt complexes of the ubiquitin mutants E24H/A28H and A28H/D32H at a ^{1}H NMR frequency of 800 MHz. Comparison of the experimental RDCs with RDCs predicted by the PCS-derived $\Delta\chi$ tensors using Equation (1) yielded excellent correlations (Figure 3c,d). The best quality factors (0.21) were obtained for the structure ensemble 2KOX[23] (Table S2). This structure ensemble has previously been identified to produce the best fit to PCSs generated by lanthanide tags.[24] A free fit of the alignment tensors to the structure ensemble improved the quality factors only a little (to 0.18) and closely reproduced the Euler angles of the $\Delta\chi$ tensors (Table 1). The close agreement between the $\Delta\chi$ tensors determined from PCSs and RDCs confirms the excellent definition of the metal position by the dHis motif. In previous reports of proteins labeled with Co^{2+} tags, $\Delta\chi$ tensors derived from RDCs were consistently smaller than the $\Delta\chi$ tensors derived from PCSs,[20,25] thus suggesting non-unique locations of the metal ion relative to the protein.[5]

Table 1: $\Delta\chi$ tensor parameters of ubiquitin mutants E24H/A28H and A28H/D32H derived from either PCSs or RDCs.[a]

		$\Delta\chi_{ax}$	$\Delta\chi_{rh}$	Euler angles		
		10^{-32} m^3	10^{-32} m^3	α/°	β/°	γ/°
E24H/A28H	PCS	−3.8	−2.0	45	160	57
	RDC	−3.9	−2.2	53	162	61
A28H/D32H	PCS	−3.7	−0.4	156	82	29
	RDC	−3.6	−0.4	154	86	31

[a] Setting the ^{1}H–^{15}N bond lengths to 1.008 Å to fit the alignment tensor.[26] The tensors were fitted to residues 1–70 of the structure ensemble published under PDB ID: 2KOX.[23]

The high fidelity of the metal position achieved by the dHis motif was confirmed by modeling. For both the α-helical and the β-sheet dHis motifs, only a single conformation of the histidine side chains could be found when the position of the Co^{2+} ion was constrained to the planes of both imidazole rings and the nitrogen–cobalt bond length to 2 Å. The models of the α-helical dHis motifs showed dihedral angles χ_1 near 180° and −60° for the histidine residues in positions i and $i+4$, respectively. These constraints resulted in bond angles between the two nitrogen–cobalt bonds of about 60° for the ubiquitin mutants. The modeled metal positions were always near the position determined by PCSs. Although the modeled conformations in the ubiquitin E24H/A28H and A28H/D32H mutants were very similar, the experimentally determined $\Delta\chi$ tensors showed very different orientations relative to the α-helix (Figure 3e,f), thus indicating sensitivity to very small changes in the ligand field of the Co^{2+} ion. Sensitivity of $\Delta\chi$ tensor parameters with regard to the coordinating chemical groups and their geometry is well known for established Co^{2+} tags.[20,25]

In the case of the β-strand dHis motif of GB1 E15H/T17H, the metal position indicated by the PCSs deviated more strongly from the position modeled with the α-helical dHis constraints, which may be explained by a different χ_1 rotamer of the histidine residue in position $i+4$ (Figure S4 and Table S4). We speculate that the smaller $\Delta\chi$ tensor observed for the dHis motif in GB1 and the lesser quality factor associated with the $\Delta\chi$ tensor fit reflects transient dissociation of the Co^{2+} complex, as suggested by the weaker binding of the Co^{2+} ion to GB1 E15H/R17H (Figure S1). The differences in binding affinities between α-helical and β-strand dHis motifs were also evident during protein purification, where the GB1 mutant eluted from the Ni-NTA column at about 60 mM imidazole whereas the ubiquitin mutants eluted at about 250–300 mM imidazole.

The affinity of histidine for Zn^{2+} is only little less than for Co^{2+} ions, but titration with $ZnCl_2$ resulted in protein precipitation at the concentrations needed for ITC. Although the [^{15}N,^{1}H]-HSQC spectra were very similar in the presence and absence of $ZnCl_2$, good $\Delta\chi$ tensor fits required PCS data using zinc for the diamagnetic reference, thus suggesting that dHis-Zn^{2+} and dHis-Co^{2+} motifs share the same structure. Due to the relatively weak binding affinity of Co^{2+} and Zn^{2+} ions to the dHis motif, measurements at low protein concentration may feature cross-peaks from both metal-bound and metal-free species. In this case the resulting increase in spectral overlap may need to be resolved by 3D NMR spectra such as HNCO spectra. While the dHis motif was furnished with the Cu^{2+}-IDA complex for earlier EPR work,[12,13] using solutions of $CoCl_2$ and IDA or NTA premixed in a 1:1 ratio did not generate PCSs in the ubiquitin or GB1 mutants.

The dHis-Co^{2+} motif provides the most rigid metal-binding site reported for proteins and it can be engineered by changing only two amino acid residues. PCSs produced by the dHis-Co^{2+} motif are uniquely capable of delivering structure restraints of exceptional quality. The paramagnetic shifts can be measured conveniently by exchange experiments. The α-helical dHis motif can reliably be introduced into proteins of unknown three-dimensional structure, since solvent-exposed α-helices are readily identified from amino acid sequences by their amphiphilic character. The dHis-Co^{2+} motif is compatible with solvent-exposed cysteine residues (Figure S5). dHis motifs are inexpensive to implement by simple mutation and allow affinity protein purification without an additional His-tag. These properties render the dHis motif superior to the incorporation of unnatural Co^{2+}-binding amino acids[27] or other histidine motifs, which do not immobilize the metal ion very well and are suitable only for the generation of PREs.[28] PCS measurements with the α-helical dHis-Co^{2+} motif present a precision tool for protein structure determination and analysis by NMR spectroscopy.

Acknowledgements

We thank Henry Orton for help with resonance assignments of GB1. Mass spectrometry experiments were performed at the Australian National University Research School of Chemistry/Research School of Biology Joint Mass Spectrometry Facility under the supervision and guidance of Dr. Adam J. Carroll. Financial support by the Australian Research Council, including a Laureate Fellowship to G. O., is gratefully acknowledged.

Conflict of interest

The authors declare no conflict of interest.

Keywords: I_zS_z-exchange spectra · NMR spectroscopy · protein structures · pseudocontact shifts · residual dipolar coupling

How to cite: *Angew. Chem. Int. Ed.* **2018**, *57*, 6226–6229
Angew. Chem. **2018**, *130*, 6334–6337

[1] G. Otting, *Annu. Rev. Biophys.* **2010**, *39*, 387–405.
[2] C. Nitsche, G. Otting, *Prog. Nucl. Magn. Reson. Spectrosc.* **2017**, *98*, 20–49.
[3] X. C. Su, G. Otting, *J. Biomol. NMR* **2010**, *46*, 101–112.
[4] C. T. Loh, K. Ozawa, K. L. Tuck, N. Barlow, T. Huber, G. Otting, B. Graham, *Bioconjugate Chem.* **2013**, *24*, 260–268.
[5] D. Shishmarev, G. Otting, *J. Biomol. NMR* **2013**, *56*, 203–216.
[6] M. A. Hass, P. H. J. Keizers, A. Blok, Y. Hiuma, M. Ubbink, *J. Am. Chem. Soc.* **2010**, *132*, 9952–9953.
[7] A. P. Welegedara, Y. Yang, M. D. Lee, J. D. Swarbrick, T. Huber, B. Graham, D. Goldfarb, G. Otting, *Chem. Eur. J.* **2017**, *23*, 11694–11702.
[8] K. Barthelmes, A. M. Reynolds, E. Peisach, H. R. A. Jonker, N. J. DeNunzio, K. N. Allen, B. Imperiali, H. Schwalbe, *J. Am. Chem. Soc.* **2011**, *133*, 808–819.
[9] D. Barthelmes, M. Gränz, K. Barthelmes, K. N. Allen, B. Imperiali, T. Prisner, H. Schwalbe, *J. Biomol. NMR* **2015**, *63*, 275–282.
[10] F. H. Arnold, B. L. Haymore, *Science* **1991**, *252*, 1796–1797.
[11] J. Voss, L. Salwinski, H. R. Kaback, W. L. Hubbell, *Proc. Natl. Acad. Sci. USA* **1995**, *92*, 12295–12299.
[12] T. F. Cunningham, M. R. Putterman, A. Desai, W. S. Horne, S. Saxena, *Angew. Chem. Int. Ed.* **2015**, *54*, 6330–6334; *Angew. Chem.* **2015**, *127*, 6428–6432.
[13] M. J. Lawless, S. Ghosh, T. F. Cunningham, A. Shimshi, S. Saxena, *Phys. Chem. Chem. Phys.* **2017**, *19*, 20959–20967.
[14] Z. Liu, Z. Gong, D. C. Guo, W. P. Zhang, C. Tang, *Biochemistry* **2014**, *53*, 1403–1409.
[15] J. R. Tolman, J. M. Flanagan, M. A. Kennedy, J. H. Prestegard, *Proc. Natl. Acad. Sci. USA* **1995**, *92*, 9279–9283.
[16] N. Tjandra, A. Bax, *Science* **1997**, *278*, 1111–1114.
[17] G. Wider, D. Neri, K. Wüthrich, *J. Biomol. NMR* **1991**, *1*, 93–98.
[18] M. John, M. J. Headlam, N. E. Dixon, G. Otting, *J. Biomol. NMR* **2007**, *37*, 43–51.
[19] G. T. Montelione, G. Wagner, *J. Am. Chem. Soc.* **1989**, *111*, 3096–3098.
[20] J. D. Swarbrick, P. Ung, S. Chhabra, B. Graham, *Angew. Chem. Int. Ed.* **2011**, *50*, 4403–4406; *Angew. Chem.* **2011**, *123*, 4495–4498.
[21] H. Yagi, K. B. Pilla, A. Maleckis, B. Graham, T. Huber, G. Otting, *Structure* **2013**, *21*, 883–890.
[22] C. Schmitz, M. J. Stanton-Cook, X. C. Su, G. Otting, T. Huber, *J. Biomol. NMR* **2008**, *41*, 179–189.
[23] R. B. Fenwick, S. Esteban-Martín, B. Richter, D. Lee, K. F. Walter, D. Milovanovic, S. Becker, N. A. Lakomek, C. Griesinger, X. Salvatella, *J. Am. Chem. Soc.* **2011**, *133*, 10336–10339.
[24] B. J. G. Pearce, S. Jabar, C. T. Loh, M. Szabo, B. Graham, G. Otting, *J. Biomol. NMR* **2017**, *68*, 19–32.
[25] Y. Yang, F. Huang, T. Huber, X.-C. Su, *J. Biomol. NMR* **2016**, *64*, 103–113.
[26] L. Yao, B. Vögeli, J. Ying, A. Bax, *J. Am. Chem. Soc.* **2008**, *130*, 16518–16520.
[27] T. H. Nguyen, K. Ozawa, M. Stanton-Cook, R. Barrow, T. Huber, G. Otting, *Angew. Chem. Int. Ed.* **2011**, *50*, 692–694; *Angew. Chem.* **2011**, *123*, 718–720.
[28] M. R. Jensen, C. Lauritzen, S. W. Dahl, J. Pedersen, J. J. Led, *J. Biomol. NMR* **2004**, *29*, 175–185.

Manuscript received: February 27, 2018
Accepted manuscript online: April 6, 2018
Version of record online: April 26, 2018

